Two phase formation of massive elliptical galaxies: study through cross-correlation including spatial effect

Soumita Modak[1] • Tanuka Chattopadhyay[2] •
Asis Kumar Chattopadhyay[1]

Abstract Area of study is the formation mechanism of the present-day population of elliptical galaxies, in the context of hierarchical cosmological models accompanied by accretion and minor mergers. The present work investigates the formation and evolution of several components of the nearby massive early-type galaxies (ETGs) through cross-correlation function (CCF), using the spatial parameters right ascension (RA) and declination (DEC), and the intrinsic parameters mass (M_*) and size. According to the astrophysical terminology, here these variables, namely mass, size, RA and DEC are termed as parameters, whereas the unknown constants involved in the kernel function are called hyperparameters. Throughout this paper, the parameter size is used to represent the effective radius (R_e). Following Huang et al. (2013a), each nearby ETG is divided into three parts on the basis of its R_e value. We study the CCF between each of these three components of nearby massive ETGs and the ETGs in the high redshift range, $0.5 < z \leq 2.7$. It is found that the innermost components of nearby ETGs are highly correlated with ETGs in the redshift range, $2 < z \leq 2.7$, known as 'red nuggets'. The intermediate and the outermost parts have moderate correlations with ETGs in the redshift range, $0.5 < z \leq 0.75$. The quantitative measures are highly consistent with the two phase formation scenario of nearby massive ETGs, as suggested by various authors, and resolve the conflict raised in a previous work (De, Chattopadhyay, & Chattopadhyay 2014) suggesting other possibilities for the formation of

Soumita Modak

Tanuka Chattopadhyay

Asis Kumar Chattopadhyay

[1]Department of Statistics, University of Calcutta, 35 B.C. Road, Kolkata 700019, India.

[2]Department of Applied Mathematics, University of Calcutta, 92 A.P.C Road, Kolkata 700009, India.

the outermost part. A probable cause of this improvement is the inclusion of the spatial effects in addition to the other parameters in the study.

1 Introduction

Hubble (1934) first studied the frequency distribution of galaxies according to their positions (i.e. RA and DEC) in the universe and the distribution of pairwise distances was found to be strongly skewed, which indicates that the galaxies have spatial clustering nature. The clustering nature is intrinsic compared to uniform distribution (Bok 1934; Mowbray 1938). Numerous studies have been carried out to explore the clustering nature using position coordinates (viz. RA and DEC) (Chandrasekhar & Munch 1952; Zwicky 1933; Limber 1953, 1954; Neyman, Scott, & Shane 1954). De, Chattopadhyay, & Chattopadhyay (2014) investigated the clustering nature with respect to the intrinsic properties of the galaxies through mass and size.

The discovery of compact massive ETGs at high redshift has raised questions on the plausible formation mechanisms for the present-day population of elliptical galaxies from the classical view of a single event, e.g. monolithic collapse (Larson 1975; Carlberg 1984; Arimoto & Yoshii 1987) or a major merger (Toomre, & Toomre 1972; Ashman & Zepf 1992; Zepf et al. 2000; Bernardi et al. 2011; Prieto et al. 2013). Instead, the single events have to be embedded in hierarchical merging, called minor mergers accompanied by continuous accretion (Forbes, Bordie, & Grillmair 1997; Jeong et al. 2007; Mondal, Chattopadhyay, & Chattopadhyay 2008; Kaviraj et al. 2011; Bluck, Conselice, & Buitrago 2012; Newman et al. 2012; Shabala et al. 2012, 2017).

Interested readers may also consult the references listed in these papers. Recent discovery of compact high redshift galaxies (Daddi, Renzini, & Pirzkal 2005; Cappellari et al. 2009; Damjanov et al. 2011; Onodera et al. 2012) and intermediate redshift galaxies, having stellar masses and sizes increased by a factor of $3 - 4$ (van Dokkum et al. 2010; Papovich et al. 2012; Szomoru, Franx, & van Dokkum 2012), suggests two phase formation of nearby massive ETGs (Oser et al. 2010; Forbes et al. 2011; Gobat et al. 2011; van Dokkum et al. 2015; de la Rosa et al. 2016; Vulcani et al. 2016). First, an intense dissipational process like accretion (Dekel, Sari, & Ceverino 2009) or major merger forms an initially compact inner part, then a slower phase starts when the outermost part is developed through non-dissipational process, e.g. dry merger. This two phase model (Oser et al. 2010; Johansson, Naab, & Ostriker 2012) severely challenges the classical 'single event' model. Huang et al. (2013b) explored the two phase theory through matching 'median' values of the two systems, which suffers from the following limitations. They have considered only univariate data like 'mass' or 'size' at a time. The present study shows that the ETGs in the redshift range, $0.5 < z \leq 2.7$, have estimated correlation (Pearson product-moment correlation coefficient) between mass and size as $r_p = 0.348$, with $p-$value $\simeq 0$ for testing the null hypothesis H_0 : correlation between mass and size is zero against the alternative H_1 : correlation between mass and size is non-zero. Three components of nearby ETGs (defined in Section 2) have estimated correlations as $r_p = 0.817$, $r_p = 0.623$ and $r_p = 0.668$ respectively, and each has $p-$value $\simeq 0$ for the above test. It indicates that mass and size of the ETGs are correlated and hence the use of univariate median matching is not suitable for them. Also, median causes loss of information, as it does not directly use all the observations of a given data set. But, bivariate study of mass and size through CCF (De, Chattopadhyay, & Chattopadhyay 2014) suggested three phase formation of nearby massive ETGs. To solve this conflict, we study the CCF by combining the intrinsic parameters mass and size with the spatial effects RA and DEC. As mass-size bivariate data are significant for exploring intrinsic clustering nature and spatial coordinates are significant for spatial clustering, we combine the above two to study the interaction between them.

The present work computes the CCF between the different components of nearby massive ETGs and the high redshift ($0.5 < z \leq 2.7$) ETGs. To find the distances between the ETGs, we consider the Euclidean norm, which is suitable for linear parameters like mass and size, but cannot be used for angular parameters like RA and DEC. As our study includes both types of parameters, we consider the Euclidean metric based on mass, size, linearized RA (say, RA_l) and linearized DEC (say, DEC_l), in which values of RA and DEC are linearized throughout the analysis. Here, due to noisy or sparsely distributed ETGs, the raw data cannot be used in studying the CCF. Hence, we compute the CCF, using the relevant information in terms of the kernel principal components (KPCs). Here the KPCs are extracted from the ETGs through kernel principal component analysis (KPCA) with the help of the positive definite kernel proposed in Modak, Chattopadhyay, & Chattopadhyay (2017). It gives the result which is highly consistent with the two phase formation scenario of nearby massive ETGs. It also resolves the conflict raised in a previous work (De, Chattopadhyay, & Chattopadhyay 2014) suggesting other possibilities for formation of the outermost part of nearby massive ETGs. The paper is organized as follows. In Section 2, we discuss the data sets whereas Section 3 describes the methods. The results and discussion are given in Section 4.

2 Data sets

In Huang et al. (2013a), a nearby ETG is divided into three parts defined as the inner component with $R_e \leq 1$ kpc, the intermediate component with $R_e \sim 2.5$ kpc, and the outermost component with $R_e \sim 10$ kpc. Let the effective radii and the masses for these three parts be denoted by $R_{e,1}, R_{e,2}, R_{e,3}$ and $M_{*,1}, M_{*,2}, M_{*,3}$ respectively. Here each galaxy has unique values for RA and DEC (regardless of its different parts), which are transformed from angular form to linear form (see, Subsection 3.1, for details of the transformation method) for our study. Thus, we have data for 70 nearby massive ($M_* > 10^8 M_\odot$) ETGs on eight parameters, namely $R_{e,1}$, $R_{e,2}$, $R_{e,3}$, $M_{*,1}$, $M_{*,2}$, $M_{*,3}$, RA_l and DEC_l. Now, to include the spatial effect in the study, we first cluster these 70 ETGs, based on the above-mentioned eight parameters, into three clusters. Here, for clustering we use the k-medoids clustering method based on the Euclidean distance (Kaufman, & Rousseeuw 1990). It results in the first cluster with the minimum value for $< R_{e,1} >$ ($< R_{e,1} >=$ arithmetic mean of observations on $R_{e,1}$), the second cluster with medium value for $< R_{e,2} >$ and the third cluster with the maximum value for $< R_{e,3} >$. Then, we choose $R_{e,1}, M_{*,1}, RA_l$, DEC_l values for the ETGs from the first cluster denoted as data set 1, which represents the innermost part of the nearby ETGs. Next, we consider $R_{e,2}, M_{*,2}, RA_l$, DEC_l observations for the second cluster which form data set 2, representing the intermediate part. Lastly,

data set 3 includes $R_{e,3}$, $M_{*,3}$, RA_l, DEC_l values from the third cluster which denotes the sample from the outermost part. Thus, data sets $1-3$ of sizes $15, 25$ and 30 respectively, have observations on four parameters mass, size, RA_l and DEC_l. Depending on the division of Re, i $(i = 1, 2, 3)$ value in three groups, there may be 27 different combinations as each Re, i $(i = 1, 2, 3)$ can be chosen in 3 ways, although some combinations might not give rise to significant variations in the CCF. In order to check for the robustness of our results which depend upon the chosen representative samples, we have also considered other distinct choices for data sets $1-3$ and obtained similar results.

For comparison, we collect data on mass, size, RA_l, DEC_l for 1012 ETGs in the high redshift range (viz. $0.5 < z \le 2.7$) from the following sources. 364 ETGs $(0.50 < z \le 2.67)$ from Damjanov et al. (2011), 248 ETGs $(1.49 \le z \le 1.79)$ from Papovich et al. (2012), 142 ETGs $(0.70 \le z \le 1.31)$ from Chen et al. (2013), 177 ETGs $(0.52 \le z \le 2.35)$ from Szomoru et al. (2013) and 81 ETGs $(1.28 \le z \le 1.50)$ from McLure et al. (2013). These data sets $4-8$ of respective sizes $168, 218, 206, 391$ and 29, contain massive ellipticals (with $M_* > 10^8 M_\odot$) in the redshift zones (defined similarly as in De et al. (2014)) $0.5 < z \le 0.75$, $0.75 < z \le 1$, $1 < z \le 1.4$, $1.4 < z \le 2$ and $2 < z \le 2.7$ respectively.

3 Method

3.1 Linearization of angular data

As we consider the Euclidean distance in estimating the CCF, we transform the angular data on RA and DEC into some linear form by the help of the method proposed in Chattopadhyay, Mondal, & Biswas (2015). Let θ be the angular data with the unique mode ϕ, then its linear form is given by $1 - cos(\theta - \phi)$. If θ has two modes ϕ_1 and ϕ_2, then its linear form is given by $max\{1 - cos(\theta - \phi_1), 1 - cos(\theta - \phi_2)\}$. Now, mode of θ can be estimated from its histogram, in which the circumference of the circle is split into groups specified by bins and the radii of the corresponding sectors are computed as equal to the square root of the relative frequencies of observations in each group. For example, see Fig. 1, the histogram of RA for the ETGs in the redshift zone $0.5 < z \le 0.75$, i.e. data set 4, indicates a bimodal distribution with $\phi_1 \sim 45°$ and $\phi_2 \sim 180°$. Similarly, the histogram of DEC for data set 4 (Fig. 2) indicates its unimodal density with $\phi \sim 0°$.

3.2 Compatibility test

Since the data sets $4 - 8$ have different sources, they obviously suffer from selection biases and errors. Hence, compatibility test is necessary before combining them into a study. So, we perform the Duda-Hart test (Duda & Hart 1973), for each of the four parameters, to check homogeneity between two data sets from different sources (Table 1). The test is performed for data sets within the same redshift zone, as the galaxies have undergone cosmological evolution via merger and accretion (Khochfar, & Silk 2006; De Lucia, & Blaizot 2007; Guo & White 2008; Kormendy et al. 2009; Hopkins, Croton, & Bundy 2010; Naab 2013). Data from Damjanov et al. (2011) contains the maximum number of galaxies within the entire redshift zone ($0.5 < z \le 2.7$). So, we perform the testing between the above-mentioned data set and the other sets. It is clear from Table 1 that all the tests are accepted at 5% level of significance with high or moderate $p-$values. Hence, we assume that the combined data sets are compatible with each other with respect to the four parameters size, mass, RA_l and DEC_l.

3.3 Completeness test

For testing completeness of the combined data sets $4-8$, we use the V/V_{max} test. The test was first used by Schmidt (1956) for studying the space distribution of a complete sample of radio quasars. Let F_m be the limiting flux within maximum distance r_m and r be the radial distance of a quasar. Let us also define $V(r)$ and V_{max} as $V(r) = \frac{4\Pi r^3}{3}$ and $V_{max} = \frac{4\Pi r_m^3}{3}$. Then, if all the quasars follow a uniform distribution over the entire range of observation, V/V_{max} will be uniformly distributed over $[0, 1]$ with $< V/V_{max} >= 0.5$. We obtain $< log|R_e|/log|R_{e,max}| >= 0.445$ (removing 65 outliers), $< log|M|/log|M_{max}| >= 0.862$, $< logRA/logRA_{l,max} >= 0.537$ and $< logDEC/logDEC_{l,max} >= 0.363$ (removing 145 outliers) (here, suffix 'max' represents the maximum value of the corresponding parameter). As the mean values for all the parameters, except mass, are close to 0.5, we can conclude that the combined data set is complete in 75% (i.e. 3 out of 4) of its parameters.

This method involves only point estimation of the expectation of Uniform $(0, 1)$ by its sample mean, which is always affected by outliers. Here, by outliers we mean the observations which are "far away" from the average value of the remaining observations. Hence, a parallel nonparametric test, which is unaffected by outliers, is also preferred. So, we check completeness by performing the Kolmogorov-Smirnov test

(Kolmogorov 1933; Corder, & Foreman 2014) for the following testing problems with H_{01}: Distribution of $logR_e/logR_{e,max}$ is Uniform over $[-1, 1]$, H_{02}: Distribution of $logM/logM_{max}$ is Uniform over $[-1, 1]$, H_{03}: Distribution of $logRA_l/logRA_{l,max}$ is Uniform over $[0, 1]$, and H_{04}: Distribution of $logDEC/logDEC_{l,max}$ is Uniform over $[0, 1]$, for each of which the alternative is "the null hypothesis does not hold". The $p-$values for all the above tests came out to be almost zero, which proves that the combined data set is complete. For comparison, we also plot the combined data sets $1-3$ and $4-8$ in the mass-size plane (Figs. 3 and 4 respectively) and in the $RA_l - DEC_l$ plane (Figs. 5 and 6 respectively).

3.4 Cross-correlation function (CCF)

The theory of the CCF (ξ) was first introduced by Neyman, & Scott (1952) for studying galaxy clustering on the basis of four assumptions, namely (i) galaxies have a natural tendency to occur in groups, (ii) the number of galaxies varies in each group following certain probabilistic law, (iii) the galaxies in each group also follow certain probabilistic distribution, and (iv) group centers in space follow quasi-uniform distribution. Subsequently, the above theory has been discussed by several authors, e.g. Peebles (1980); Martínez, & Saar (2002); Blake et al. (2006); De, Chattopadhyay, & Chattopadhyay (2014), etc. We consider the following estimator of the CCF (Blake et al. 2006) as,

$$\hat{\xi}(d) = \frac{D_1D_2(d) - D_1R_2(d) - D_2R_1(d) + R_1R_2(d)}{R_1R_2(d)}, \tag{1}$$

where d denotes the distance computed between each of the unique pairs of galaxies in two data sets. $D_1D_2(d)$ denotes a pair count between the observed data sets D_1 and D_2, i.e. frequency corresponding to a bin with separations of $d \pm \delta d/2$ in the histogram of d. Let R_i denotes the unclustered sample drawn from the data set $D_i, i = 1, 2$. Then, $D_iR_j(d)$ denotes pair count between data sets D_i and R_j, $i, j = 1, 2$ but $i \neq j$, and $R_1R_2(d)$ denotes pair count between data sets R_1 and R_2.

In our study, $\hat{\xi}$ is computed, based on mass, size, RA_l and DEC_l, where d is the normalized Euclidean distance computed between each of the unique pairs of galaxies in two data sets. But, due to noisy or sparsely distributed data, $\hat{\xi}$ shows absurd patterns, e.g. the CCF plot (plot of $\hat{\xi}(d)$ versus d) shows randomly changing inflection, or $|\hat{\xi}(d)|$ shows an overall increasing trend against d rather than decreasing, which are not physically interpretable. This can happen when the data gets contaminated with noise and hence does not reveal the inherent useful information, or the galaxies in data sets are distributed in very different ways over the survey area. In this situation, the estimated CCF becomes useless. To overcome this problem, we perform KPCA (Schölkopf, & Smola 2002) on the data sets (see, Section 3.5). Then, we consider the KPCs as our study parameters, which are used to compute $\hat{\xi}$.

3.5 Kernel principal component analysis (KPCA)

Given M observations $x_k, k = 1, 2, ..., M$, on N parameters, i.e. $x_k \in R^N$, KPCA is performed on a dot product space F by using a map from R^N to F defined as,

$$\Phi : R^N \to F.$$

Then, for $\sum_{k=1}^{M} x_k = 0$, we need to solve the following equation for eigenvalues $\lambda \geq 0$ and non-zero eigenvectors $V \in F$

$$\lambda V = \bar{C}V, \; where \; \bar{C} = \frac{1}{M}\sum_{j=1}^{M} \Phi(x_j)\Phi(x_j)^T.$$

The above-mentioned problem eventually boils down to solving the eigen value problem for the kernel matrix $K = ((K_{ij}))_{i,j=1(1)M}$ as follows (for details, see, Schölkopf, & Smola (2002)),

$$M\lambda\alpha = K\alpha,$$

where $K_{ij} = < \Phi(x_i), \Phi(x_j) > (< \cdot, \cdot >$ represents the usual dot product) is a positive definite (pd) kernel. Let $\lambda_1 \geq \lambda_2 \geq ... \geq \lambda_M(\geq 0)$ denote the eigenvalues of K and $\alpha^1, \alpha^2, ..., \alpha^M$ be the corresponding complete set of eigenvectors, where λ_l is the last nonzero eigenvalue. Then, the $k-$th KPC corresponding to $\Phi(x)$ is given by

$$< V^k, \Phi(x) > = \sum_{i=1}^{M} \alpha_i^k < \Phi(x_i), \Phi(x) >$$
$$= \sum_{i=1}^{M} \alpha_i^k k(x_i, x), \; k = 1, 2, ..., l, \tag{2}$$

where $k(x_i, x) =$ kernel corresponding to x_i and x.
Now, the assumption $\sum_{k=1}^{M} x_k = 0$ can be relaxed by using the kernel matrix $\tilde{K} = ((\tilde{K}_{ij}))_{i,j=1(1)M}$ in the place of K, where $\tilde{K}_{ij} = (K - 1_MK - K1_M + 1_MK1_M)_{ij}, (1_M)_{ij} = M^{-1}$, for $i, j = 1, 2, ..., M$. Then, KPCA can be performed using conditionally positive definite (cpd) kernels, which include the 'pd' kernels (Hofmann, Schölkopf, & Smola 2008).

KPCA extracts the relevant nonlinear information from the raw data in terms of the KPCs. This

method is used for feature extraction, dimension reduction, classification, clustering, noise reduction, pattern recognition, etc. It has been successfully applied to supernovae clustering (Ishida 2012, 2013), image denoising (Rasmussen et al. 2012), clustering of gamma-ray bursts (Modak, Chattopadhyay, & Chattopadhyay 2017), denoising of chaotic time series (Jade et al. 2003), etc. In the present context, KPCA has been used as a transformation on the original data so that the noise can be significantly reduced and the actual information underlying the data sets can be explained in terms of the KPCs.

In our study, we use the following symmetric and 'pd' kernel (Modak, Chattopadhyay, & Chattopadhyay 2017)

$$k(x, y) = \exp(-\sum_{i=1}^{N} |\frac{x_i - y_i}{s_i}|^p), \qquad (3)$$

between $x, y \in R^N$, where p $(0 < p \le 2)$ is a tuning parameter and s_i $(> 0), i = 1, 2, ..., N$ are scale parameters, called hyperparameters.

The higher the order of the KPC, the less relevant information and the more noise are supposed to be contained in that component (Schölkopf, & Smola 2002). Hence, noise can be significantly reduced by taking into account only the first few KPCs and discarding the others, which is also shown in terms of pre-images in Schölkopf, & Smola (2002). So, we start with the first two KPCs and consider up to the first four KPCs (not exceeding the total number of parameters in the original data) as our study parameters. Here, we take s_i as the sample standard deviation corresponding to the $i-$th parameter, and vary p in a trial-and-error method. Ultimately, we choose the number of KPCs and the value of p such that we can extract sufficient relevant information from the data sets.

3.6 Algorithm to estimate the CCF

In the present study, the estimate of the CCF is computed as follows.
(i) We consider a pair of observed samples D_1 and D_2 of sizes n_1 and n_2 respectively. Here both samples have four parameters mass, size, RA_l and DEC_l.
(ii) By KPCA, the first few (say, N') KPCs are extracted, using kernel (3) with s_i = sample standard deviation corresponding to the $i-$th parameter and a specified value of p in $(0, 2]$, from D_1 and D_2, denoted by D_1' and D_2' respectively. Now, our pair of study samples are D_1' and D_2' having the KPCs as study parameters.
(iii) We compute pair count $D_1'D_2'(d)$, where d is the normalized Euclidean distance computed between each of the unique pairs of galaxies in two samples.
(iv) For each parameter (i.e. KPC), a random sample with replacement of size n_1 is drawn from the set of values of the parameter in D_1'. Then by assigning the parameter-wise random samples in random vectors, we form n_1 unclustered samples from D_1', denoted by R_1. Similarly, we obtain n_2 unclustered samples from D_2', denoted by R_2.
(v) We compute the pair counts $D_1'R_2(d)$, $D_2'R_1(d)$ and $R_1R_2(d)$.
(vi) We repeat steps (iv)-(v) 100 times, i.e. draw R_1, R_2 and compute the pair counts 100 times. Then, the final values for $D_1'R_2(d)$, $D_2'R_1(d)$ and $R_1R_2(d)$ are obtained by taking the mean of the respective pair counts.
(vii) Compute $\hat{\xi}$ using formula (1), where D_1 and D_2 are replaced by D_1' and D_2' respectively.
(viii) Now, we compute $\hat{\xi}$ for 100 times and the mean of them is taken as the ultimate value of $\hat{\xi}$ and their standard error is taken as the error estimate of $\hat{\xi}$.
(ix) In step (ii), consider $N' = 2, 3, 4$ and run steps (iii)-(viii).
(x) Repeat step (ii) for different values of p, and run steps (iii)-(ix).
(xi) Steps (i)-(x) are repeated considering all unique pairs of observed samples D_1 and D_2, where D_1 corresponds to a data set from $1 - 3$ and D_2 corresponds to a data set from $4 - 8$.

4 Results and discussion

We have found significant correlation between data set 1 and data set 8 (Fig. 7), based on the first four KPCs extracted from the data sets using kernel (3) with $p = 0.1$ (s_i = sample standard deviation corresponding to the $i-$th parameter). Moderate correlation is found between data set 2 and data set 4 (Fig. 8), using the first four KPCs extracted through (3) with $p = 0.5$ from both the data sets. Study with the first four KPCs, extracted through (3) with $p = 1.5$ and $p = 0.2$ from data set 3 and data set 4 respectively, shows moderate correlation (Fig. 9). The above results indicate that the innermost components of massive ellipticals are strongly correlated with ETGs in the highest redshift range, $2.0 < z \le 2.7$, known as 'red nuggets', whereas both the 'intermediate' and the 'outermost part' are correlated with ETGs in the redshift range $0.5 < z \le 0.75$. It indicates two phase formation model of nearby massive ETGs as suggested by various authors (Khochfar, & Silk 2006; De Lucia, & Blaizot 2007; Guo & White 2008;

Kormendy et al. 2009; Hopkins, Croton, & Bundy 2010; Naab 2013).

We fit the following power law to the estimated CCF

$$\xi(d) \propto \frac{1}{d}, \quad i.e. \quad \xi(d) = Ad^{-1}, \qquad (4)$$

where A is an unknown constant. It gives us an idea of the original model, indicating correlation with $|A| > 0$ and no-correlation situation with $A = 0$ (Blake et al. 2006). We also carry out the Kolmogorov-Smirnov test (Smirnov 1948) for testing H_0: power law (4) fits the estimated CCF versus H_1: H_0 is not true. The estimated value of A and $p-$value of the above test are given in the CCF plots (see, Figs. 7-9).

Discovery of 'red nuggets' in high redshift zone has challenged the formation of massive ellipticals through a single event like monolithic collapse or major merger. Nowadays ellipticals with maximum masses are expected to undergo a number of steps rather than a single event. They are formed at $z \gtrsim 6$ through a dissipative process, and subsequently become very massive $\sim (10^{11} M_\odot)$ and compact ($R_e \sim 1$ kpc) in a very short interval of time $z \sim 2$ (Dekel, Sari, & Ceverino 2009; Oser et al. 2010, 2012). In spite of the above event, a significant fraction remains less active at $z \sim 2$. They are $4 - 5$ times less compact and 2 times less massive than their low-redshift descendants (Buitrago, Trujillo, & Conselice 2008; van Dokkum 2008; Cimatti et al. 2008; Bezanson et al. 2009; van Dokkum et al. 2010; van der Wel et al. 2011; Whitaker et al. 2012).

For the massive ellipticals in the present sample, the innermost cores (data set 1) are strongly correlated with galaxies in the highest redshift zone ($2.0 < z \leq 2.7$), and their respective median values for mass are approximately $10^{10} M_\odot$ and $10^{11} M_\odot$. Hence we can reasonably conclude that this high redshift population forms the cores of at least some, if not all (Graham, Dullo, B.T., & Savorgnam 2015; Wellons et al. 2016), of the present-day massive ellipticals. Thus massive ellipticals cannot be formed by only monolithic collapse, otherwise they would be too small and too red (van Dokkum 2008; Ferré-Mateu et al. 2012).

The formation of the intermediate (data set 2) and the outer part (data set 3) might be explained as a result of major or minor mergers (Jeong et al. 2007; Naab, Johansson, & Ostriker 2009; Kaviraj et al. 2011; Shabala et al. 2012, 2017). Let $M_j, r_j, E_j, < v_j^2 >, g_j$ and $r_{g,j}$ be respectively the mass, radius, energy, mean squared speed, density and gravitational radius of a stellar system, where $j = i, m, f$ denote three different stages of the system as the initial stage, the stage after a merger with other systems and the final stage respectively. Then

$$\frac{< v_f^2 >}{< v_i^2 >} = \frac{(1 + \eta\epsilon)}{1 + \eta}, \frac{r_{g,f}}{r_{g,i}} = \frac{(1 + \eta)^2}{1 + \eta\epsilon} \; and \; \frac{g_f}{g_i} = \frac{(1 + \eta\epsilon)^3}{(1 + \eta)^5},$$

where $\eta = M_m/M_i, \epsilon = < v_m^2 > / < v_i^2 >$. So, $\eta = 1$ implies a major merger where the size doubles. In our case, the intermediate part (data set 2) has mean radius $< R_{e,2} > \sim 2.276$ kpc which is almost 7.689 times larger than the mean radius of the innermost part $< R_{e,1} > \sim 0.296$ kpc. Hence we can conclude that the intermediate parts of nearby massive ellipticals have been formed by major mergers. The result is also consistent with previous works (Chattopadhyay et al. 2009; Chattopadhyay, Mondal, & Chattopadhyay 2013).

In the limiting case, when $< v_m^2 > \ll < v_i^2 >$ or $\epsilon \ll 1$, the size increases by a factor of 4, which implies minor merger. In our situation, $< R_{e,3} > \sim 19.554$ kpc $>> < R_{e,1} > \sim 0.296$ kpc. Also, the median of mass for the outer part is of order $10^{11} M_\odot$, which is comparable with the combined masses of few dwarf galaxies. This indicates that the outermost part of nearby massive ETGs might have been formed by several minor mergers. The combined study of intrinsic parameters with spatial effects gives a more robust picture for the two-phase formation of massive ellipticals and overcomes the conflict of three phase formation (De, Chattopadhyay, & Chattopadhyay 2014). Our result is also consistent with that of Mondal, Chattopadhyay, & Chattopa (2008), where halos of massive galaxies are found to be formed by tidal stripping of satellite dwarf galaxies.

5 Acknowledgments

References

Arimoto, N., & Yoshii, Y. 1987, Astron. Astrophys., 173, 23

Ashman, K. M., & Zepf, S. E. 1992, Astrophys. J., 384, 50

Bernardi, M., Roche, N., Shankar, F., & Sheth, R. K. 2011, Mon. Not. R. Astron. Soc., 412, L6

Bezanson, R., van Dokkum, P. G., Tal, T., et al. 2009, Astrophys. J., 697, 1290

Blake, C., Pope, A., Scott, D., & Mobasher, B. 2006, Mon. Not. R. Astron. Soc., 368, 732

Bluck, A. F. L., Conselice, C. J., & Buitrago, F. 2012, Astrophys. J., 747, 34

Bok, B. J. 1934, Bull. Harv. Obser., 895, 1

Buitrago, F., Trujillo, I., & Conselice, C. J. 2008, Astrophys. J., 687, L61

Cappellari, M., di Serego Alighieri, S., Cimatti, A., et al. 2009, Astrophys. J., 704, L34

Carlberg, R. G. 1984, Astrophys. J., 286, 403

Chandrasekhar, S., & Munch, G. 1952, Astrophys. J., 115, 103

Chattopadhyay, A. K., Chattopadhyay, T., Davoust, E., Mondal, S., & Sharina, M. 2009, Astrophys. J., 705, 1533

Chattopadhyay, A. K., Mondal, S., & Chattopadhyay, T. 2013, CSDA, 57, 17

Chattopadhyay, A. K., Mondal, S., & Biswas, A. 2015, Environ Ecol Stat, 22, 33

Chen, Z., Shu, C. G., Burgarella, D., Buat, V., Huang, J. -S., & Luo, Z. J. 2013, Mon. Not. R. Astron. Soc., 431, 2080

Cimatti, A., Cassata, P., Pozzetti, L., et al. 2008, Astron. Astrophys., 482, 21

Corder, G. W., & Foreman, D. I. 2014, "Nonparametric Statistics: A Step-by-Step Approach", Wiley: Hoboken, New Jersey

Daddi, E., Renzini, A., & Pirzkal, N., 2005, Astrophys. J., 626, 680

Damjanov, I., Abraham, R. G., Glazebrook, K., et al. 2011, Astrophys. J., 739, L44

de la Rosa, I. G., La Barbera, F., Ferreras, I., et al. 2016, Mon. Not. R. Astron. Soc., 457, 1916

Dekel, A., Sari, R., & Ceverino, D. 2009, Astrophys. J., 703, 785

De Lucia, G., & Blaizot, J. 2007, Mon. Not. R. Astron. Soc., 375,2

De, T., Chattopadhyay, T., & Chattopadhyay, A.K. 2014, Proc. Astron. Soc. Aust., 31, e047

Duda, R. O., & Hart, P. E. 1973, "Pattern Classification and Scene Analysis", Wiley: New York

Ferré-Mateu, A., Vazdekis, A., Trujillo, I., et al. 2012, Mon. Not. R. Astron. Soc., 423, 632

Forbes, D.A., Bordie, J.P., & Grillmair, C.J. 1997, Astrophys. J., 113,1652

Forbes, D.A., Spitler, L.R., Romanowsky, A.J., Brodie, J.P., & Foster, C. 2011, Mon. Not. R. Astron. Soc., 413, 2943

Graham, A.W., Dullo, B.T., & Savorgnam, G.A.D. 2015, Astrophys. J., 804, 32

Gobat, R., Daddi, E., Onodera, M., et al. 2011, Astron. Astrophys., 526, A133

Guo, Q., & White, S. D. M. 2008, Mon. Not. R. Astron. Soc., 384, 2

Ho, L. C., Li, Z.-Y., Barth, A. J., Seigar, M. S., & Peng, C. Y. 2011, Astrophys. J. Suppl. Ser., 197,21

Hofmann, T., Schölkopf, B., & Smola, A. J. 2008, Ann. Statist., 36, 1171

Hopkins, P. F., Croton, D., & Bundy, K. 2010, Astrophys. J., 724, 915

Huang, S., Ho, L. C., Peng, C. Y., Li, Z. -Y., & Barth, A. J. 2013b, Astrophys. J., 766, 47

Huang, S., Ho, L. C., Peng, C. Y., Li, Z. -Y., & Barth, A. J. 2013a, Astrophys. J., 768, L28

Hubble, E. 1934, Astrophys. J., 79, 8

Ishida, E. E. O., 2012, Proceedings of the International Astronomical Union, 10, 683

Ishida, E. E. O., & de Souza, R. S. 2013, Mon. Not. R. Astron. Soc., 430, 509

Jade, A. M., Srikantha, B.,Jayaramana, V. K., et al. 2003, Chemical Engineering Science, 58, 4441

Jeong, H., Bureau, M., Yi, S. K., Krajnović, D., & Davies, R. L. 2007, Mon. Not. R. Astron. Soc., 376, 1021

Johansson, P. H., Naab, T., & Ostriker, J. P. 2012, Astrophys. J., 754, 115

Kaufman, L., & Rousseeuw, P. J. 1990, "Finding Groups in Data: An Introduction to Cluster Analysis", Wiley: New York

Kaviraj, S., Tan, K. -M., Ellis, R. S., & Silk, J. 2011, Mon. Not. R. Astron. Soc., 411, 2148

Khochfar, S., & Silk, J. 2006, Astrophys. J., 648, L21

Kolmogorov, A. 1933, G. Ist. Ital. Attuari, 4, 83

Kormendy, J., Fisher, D. B., Cornell, M. E., & Bender, R. 2009, Astrophys. J. Suppl. Ser., 182, 216

Landy, S. D., & Szalay, A. S. 1993, Astrophys. J., 412, 64

Larson, R. B. 1975, Mon. Not. R. Astron. Soc., 173, 671

Limber, D. N. 1953, Astrophys. J., 117, 134

Limber, D. N. 1954, Astrophys. J., 119, 655

Martínez, V. J., & Saar, E. 2002, "Statistics of the Galaxy Distribution", Chapman & Hall/CRC: Boca Raton

McLure, R. J., Pearce, H. J., Dunlop, J. S., et al. 2013, Mon. Not. R. Astron. Soc., 428, 1088

Modak, S., Chattopadhyay, A. K., & Chattopadhyay, T., 2017, Communications in Statistics- Simulation and Computation, DOI: 10.1080/03610918.2017.1307393

Mondal, S., Chattopadhyay, T., & Chattopadhyay, A. K. 2008, Astrophys. J., 683, 172

Mowbray, A. G. 1938, Publ. Astron. Soc. Pac., 50, 275

Naab, T., Johansson, P. H., & Ostriker, J. P., 2009, Astrophys. J., 699, L178

Naab, T., 2013, Modelling the formation of today's massive ellipticals. The Intriguing Life of Massive Galaxies, Proceedings of the International Astronomical Union, IAU Symposium, 295, 340

Newman, A. B., Ellis, R. S., Bundy, K., & Treu, T. 2012, Astrophys. J., 746, 162

Neyman, J., & Scott, E. L. 1952, Astrophys. J., 116, 144

Neyman, J., Scott, E. L., & Shane, C. D., 1954, Astrophys. J. Suppl. Ser., 1, 269

Onodera, M., Renzini, A., Carollo, M., et al. 2012, Astrophys. J., 755, 26

Oser, L., Ostriker, J. P., Naab, T., Johansson, P. H., & Burkert, A., 2010, Astrophys. J., 725, 2312

Oser, L., Naab, T., Ostriker, J. P., & Johansson, P. H., 2012, Astrophys. J., 744, 63

Papovich C., Bassett, R., Lotz, J. M., et al. 2012, Astrophys. J., 750, 93

Peebles, P. J. E., 1980, "The Large-scale Structure of the Universe", Princeton University Press: Princeton, New Jersey

Prieto, M., Eliche-Moral, M. C., Balcells, M., et al. 2013, Mon. Not. R. Astron. Soc., 428, 999

Rasmussen P. M., Abrahamsen T. J., Madsen K. H., Hansen L. K., 2012, NeuroImage, 60, 1807

Schmidt, M., 1965, "Stars and Stellar Systems, Galactic Structure", Vol. 5, eds A. Blaauw, & M. Schmidt, University of Chicago Press: Chicago, p.513

Schölkopf, B., & Smola, A. J., 2002, "Learning with kernels: Support vector machines, regularization, optimization, and beyond", MIT Press: Cambridge, Massachusetts

Shabala, S. S., Ting, Y. -S., Kaviraj, S., Lintott, C., Crockett, R. M., Silk, J., Sarzi, M., Schawinski, K., Bamford, S. P.; Edmondson, E. 2012, Mon. Not. R. Astron. Soc., 423, 59

Shabala, S. S., Deller, A., Kaviraj, S., Middelberg, E., Turner, R. J., Ting, Y. S., Allison, J. R., & Davis, T. A. 2017, Mon. Not. R. Astron. Soc., 464, 4706

Smirnov, N. 1948, Annals of Mathematical Statistics, 19, 279

Szomoru, D., Franx, M., & van Dokkum, P. G. 2012, Astrophys. J., 749, 121

Szomoru, D., Franx, M., van Dokkum, P. G., et al. 2013, Astrophys. J., 763, 73

Toomre, A., & Toomre, J. 1972, Astrophys. J., 178, 623

van der Wel, A., Rix, H.-W., Wuyts, S., et al. 2011, Astrophys. J., 730, 38

van Dokkum, P. G. 2008, Astrophys. J., 674, 29

van Dokkum, P. G., Whitaker, K. E., Brammer, G., et al. 2010, Astrophys. J., 709, 1018

van Dokkum, P.G., Nelson, E. J., Franx, M., et al. 2015, Astrophys. J., 813, 23

Vulcani, B., Marchesini, D., De Lucia, G., et al. 2016, Astrophys. J., 816, 86

Wellons, S., Torrey, P., Ma, C.P., et al. 2016, Mon. Not. R. Astron. Soc., 456, 1030

Whitaker, K. E., van Dokkum, P. G., Brammer, G., & Franx, M. 2012, Astrophys. J., 754, L29

Zepf, S. E., Beasley, M. A., Bridges, T. J., et al. 2000, Astron. J., 120, 2928
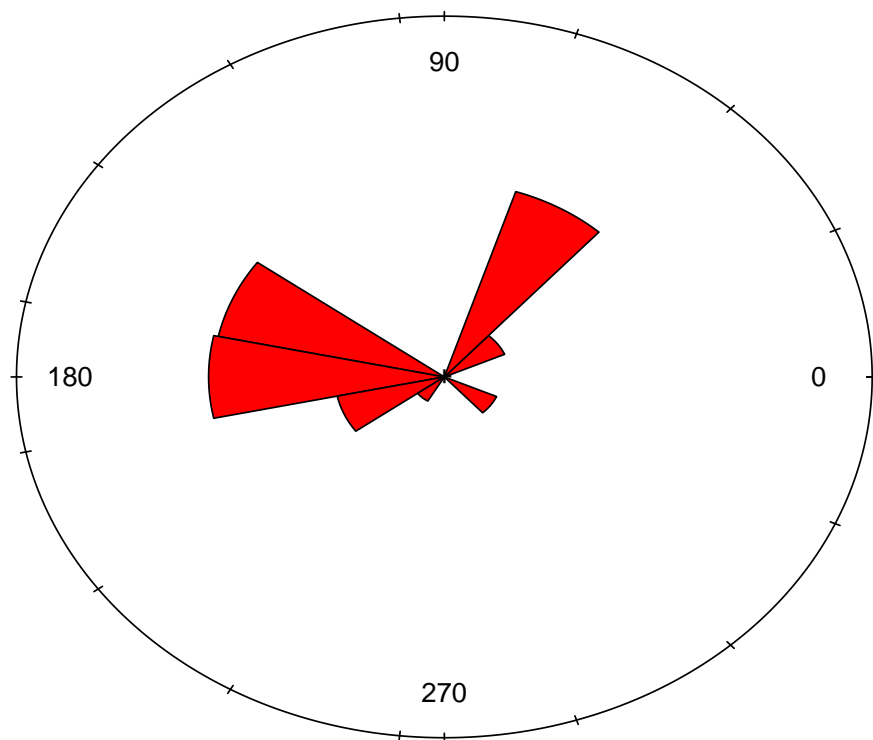
Zwicky, F. 1933, AcHPh, 6, 110

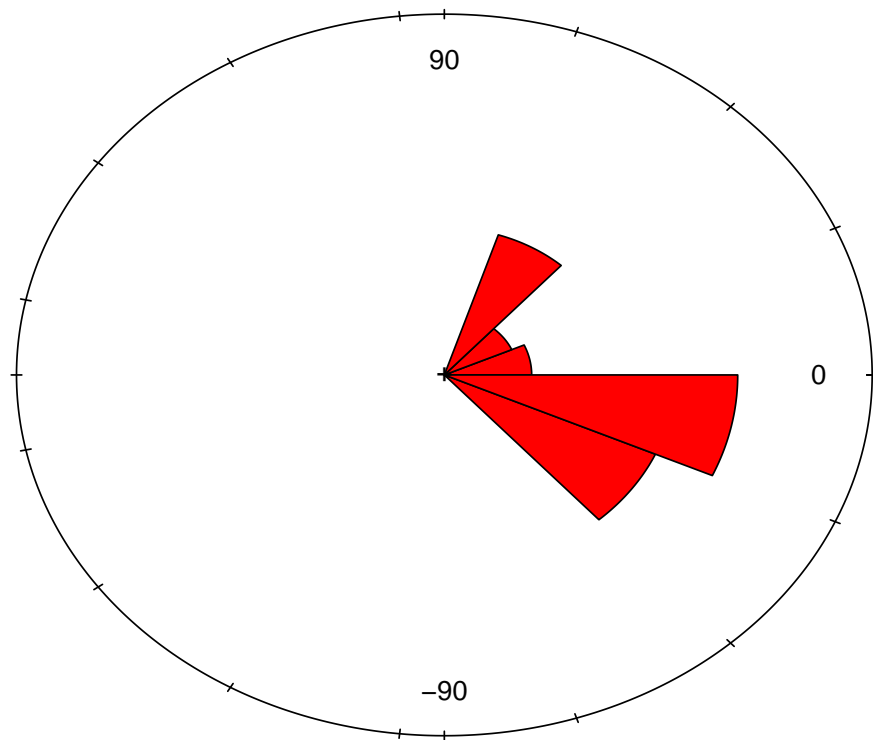**Fig. 1** Histogram of right ascension (RA) for the ETGs with $0.5 \leq z \leq 0.75$ (data set 4).

Fig. 2 Histogram of declination (DEC) for the ETGs with
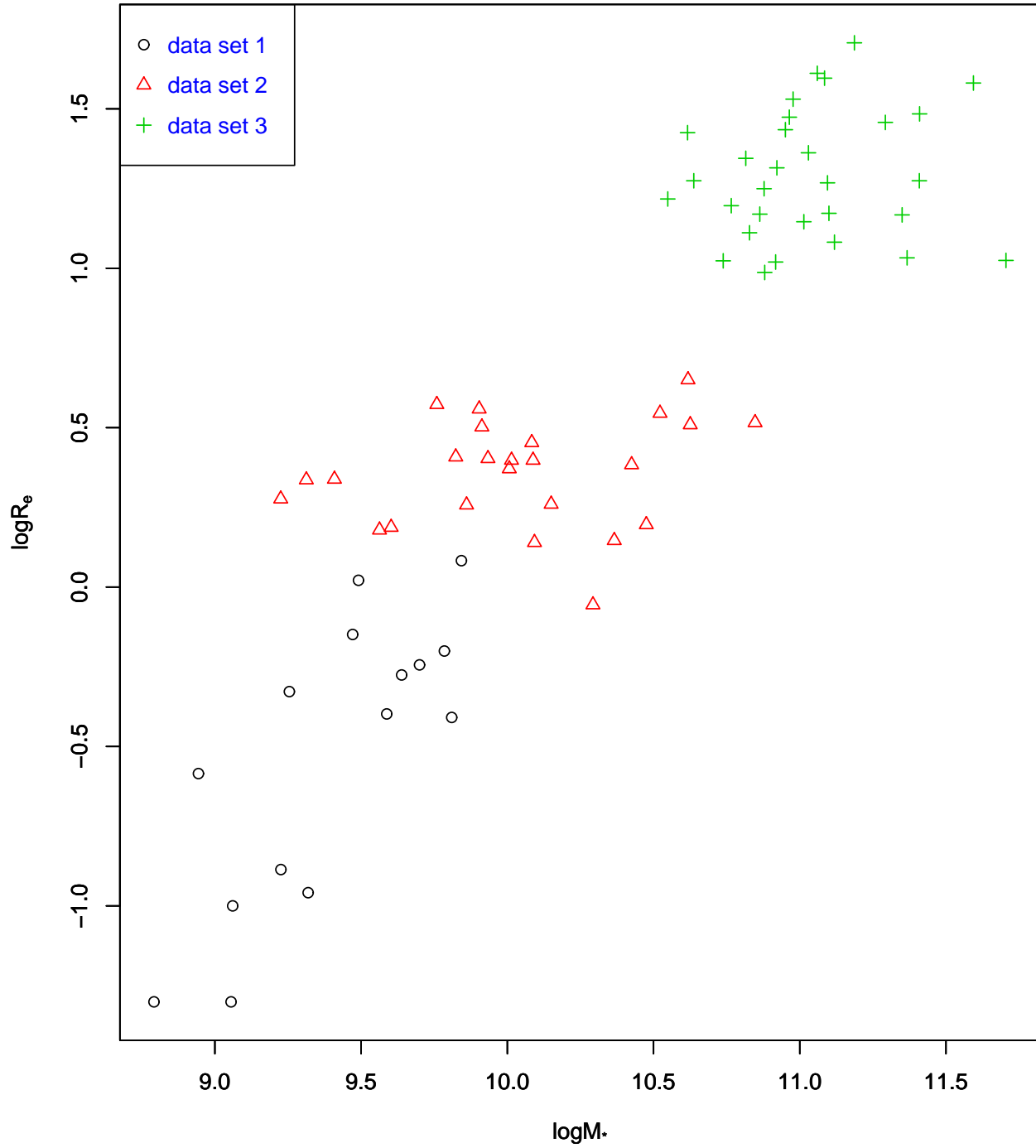$0.5 \leq z \leq 0.75$ (data set 4).

Fig. 3 Mass versus size plot for the representative samples of the three components of nearby ETGs.
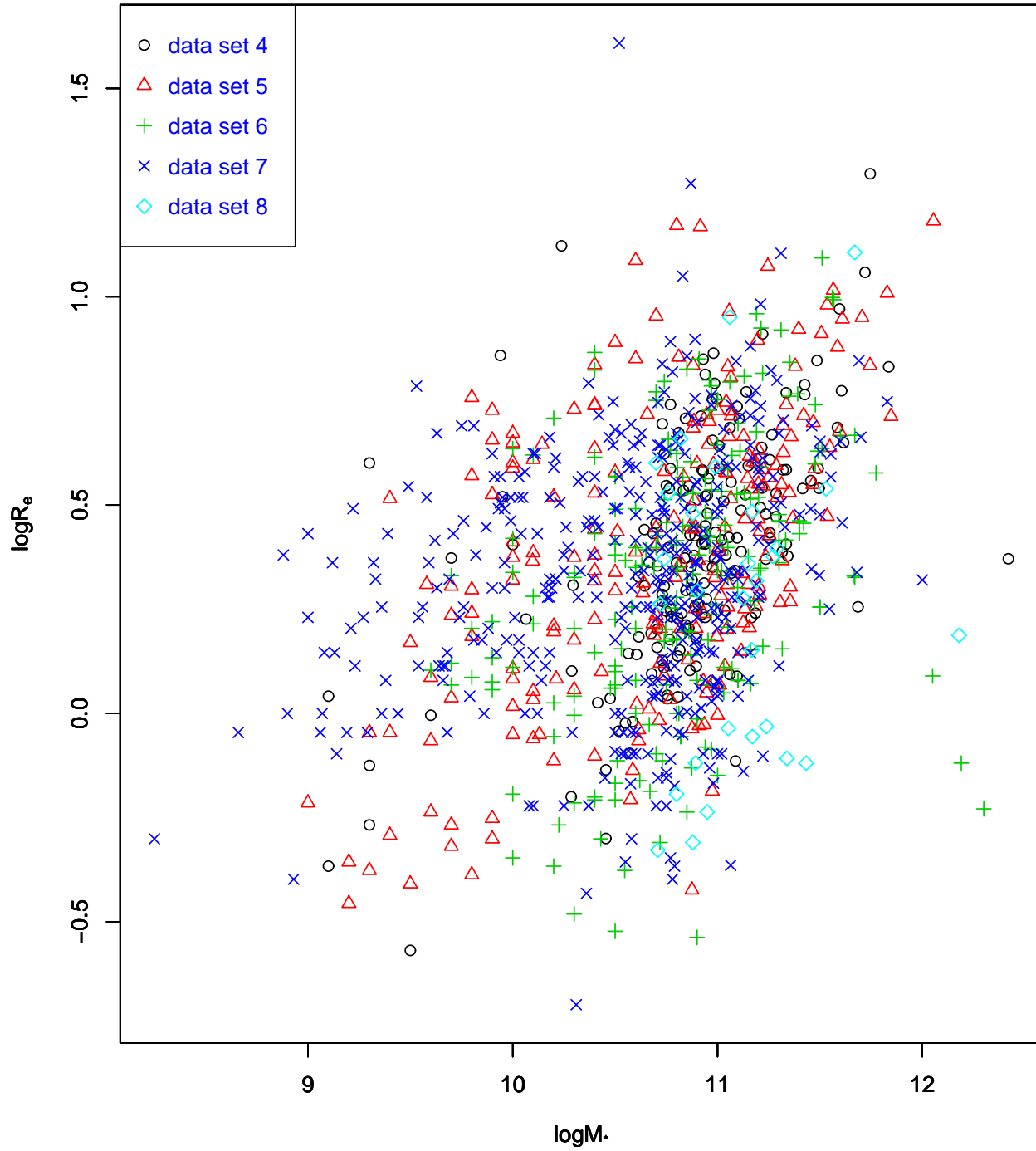
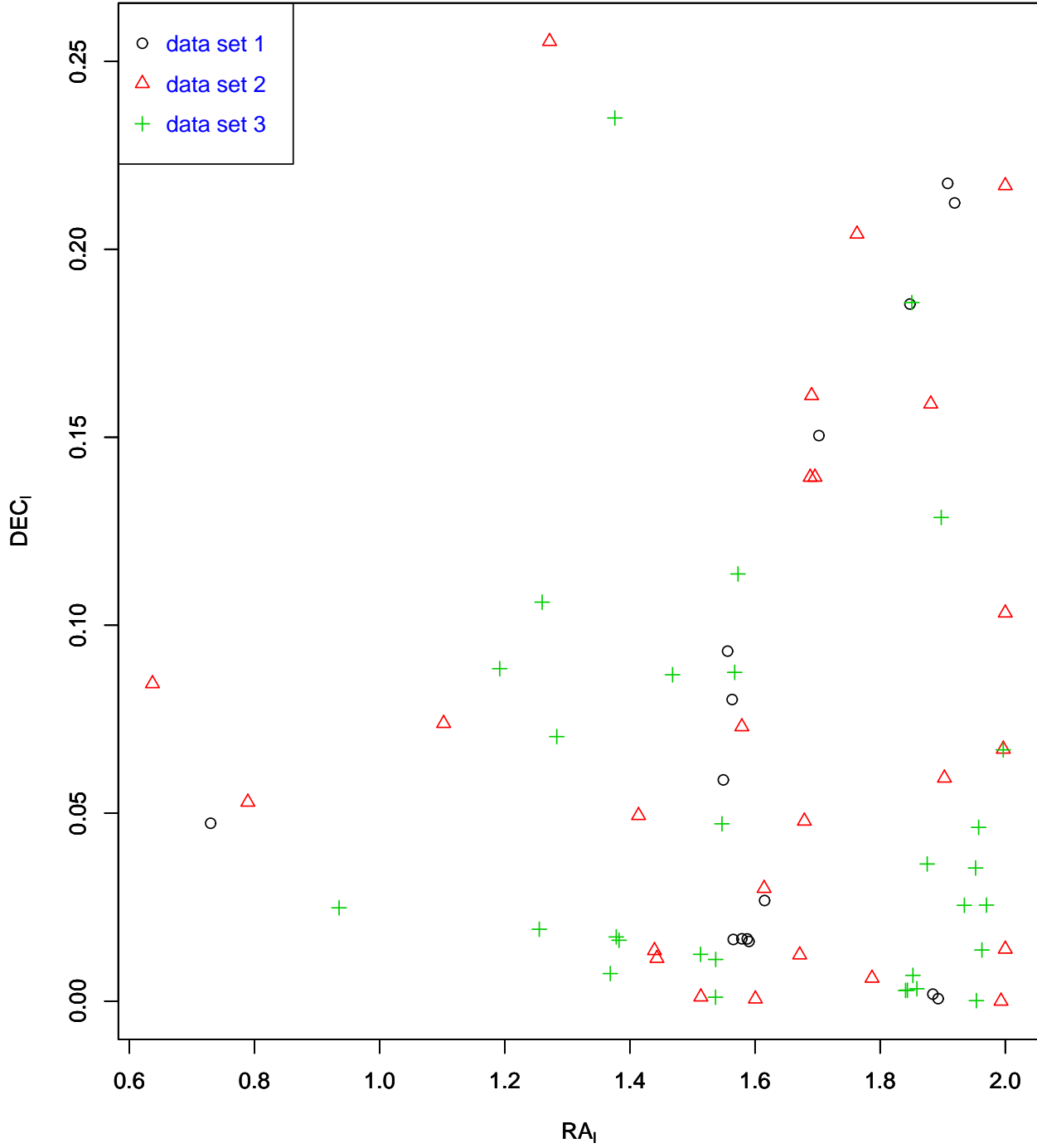**Fig. 4** Mass versus size plot for the ETGs in the high redshift zone.

Fig. 5 Linearized RA (RA_l) versus linearized DEC (DEC_l) plot for the representative samples of the three components of nearby ETGs.
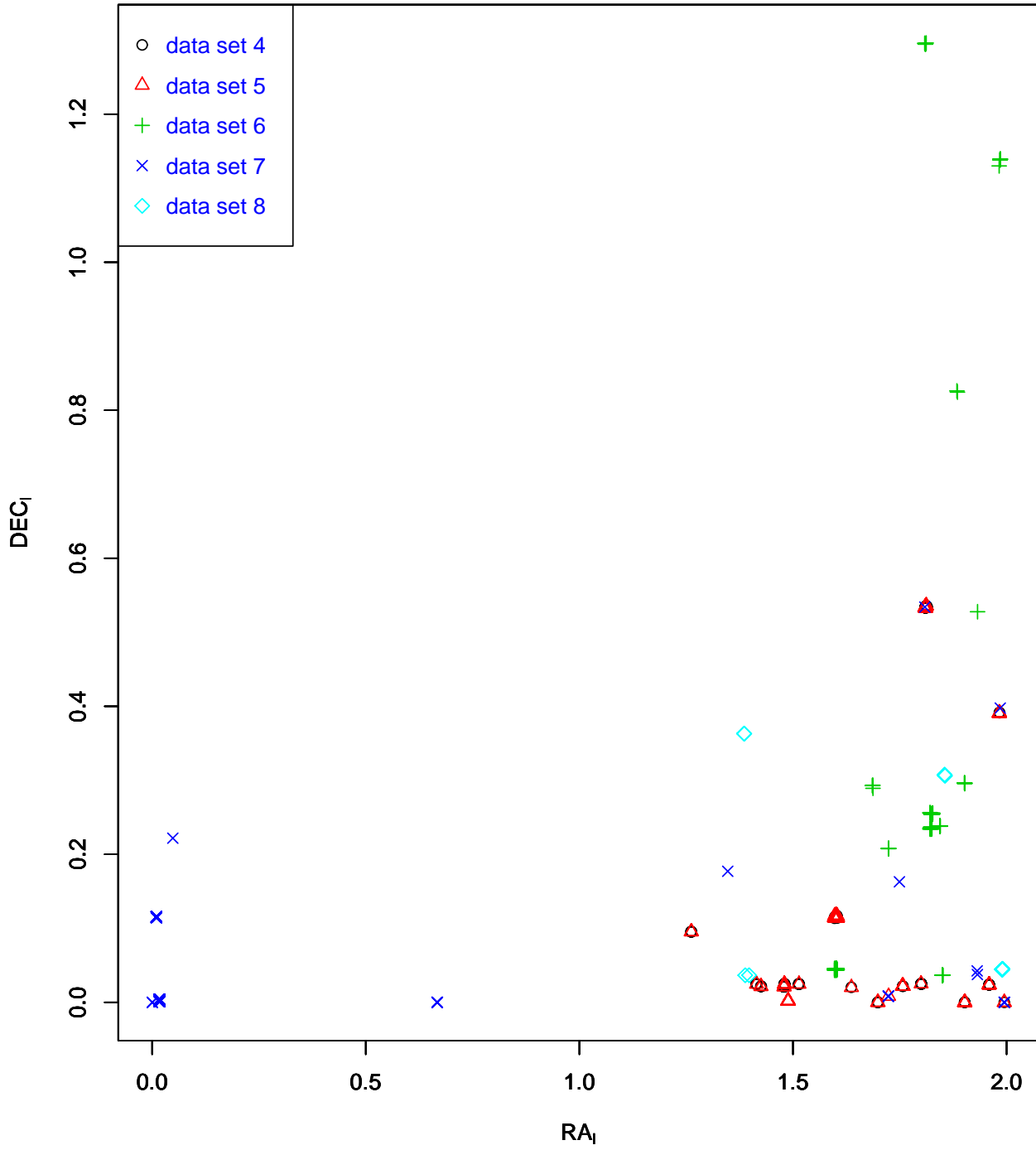
Fig. 6 RA_l versus DEC_l plot for the ETGs in the high redshift zone.
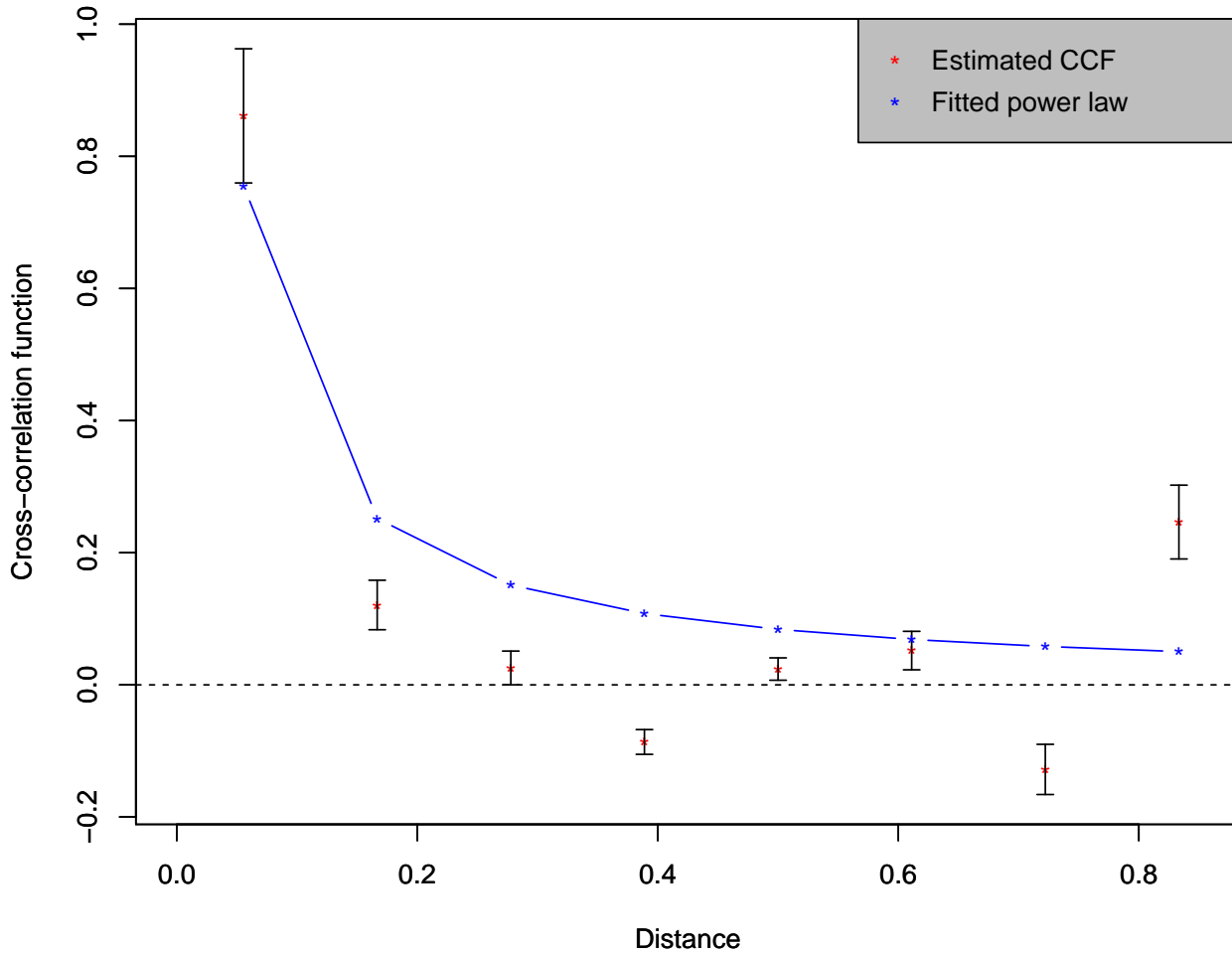
Fig. 7 Cross-correlation function (CCF) plot for the representative sample of the innermost part of nearby ETGs (data set 1) and the ETGs with $2 \leq z \leq 2.7$ (data set 8). The solid line represents the fitted power law $\xi(d) = 0.042d^{-1}$ (i.e. the estimated value of A is 0.042) and $p-$value= 0.283, corresponding to the Kolmogorov-Smirnov test for goodness of fit, indicates the fit is good.
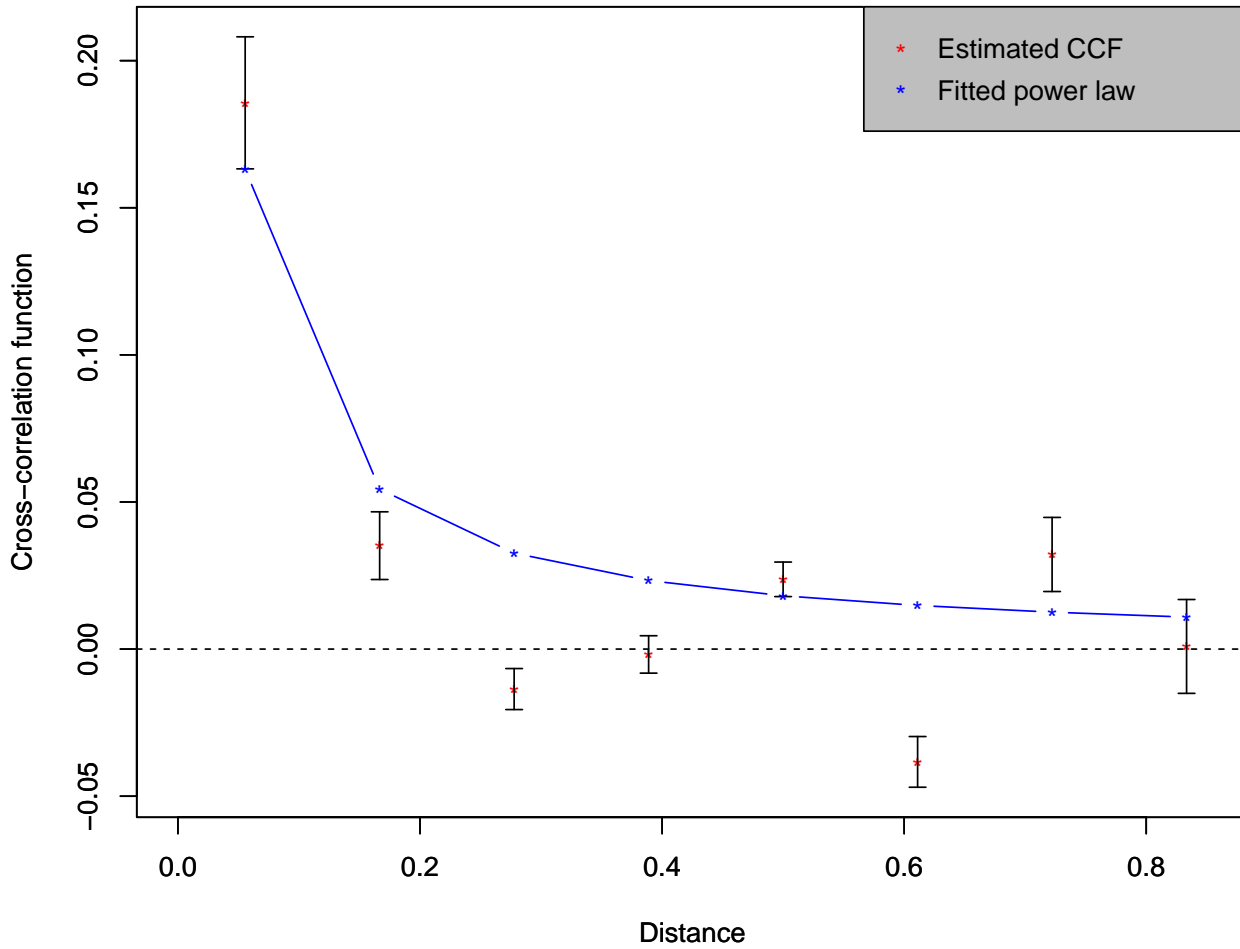
Fig. 8 CCF plot for the representative sample of the intermediate part of nearby ETGs (data set 2) and the ETGs with $0.5 \leq z \leq 0.75$ (data set 4). The solid line represents the fitted power law $\xi(d) = 0.009d^{-1}$ and $p-$value= 0.283, corresponding to the Kolmogorov-Smirnov test for goodness of fit, indicates the fit is good.
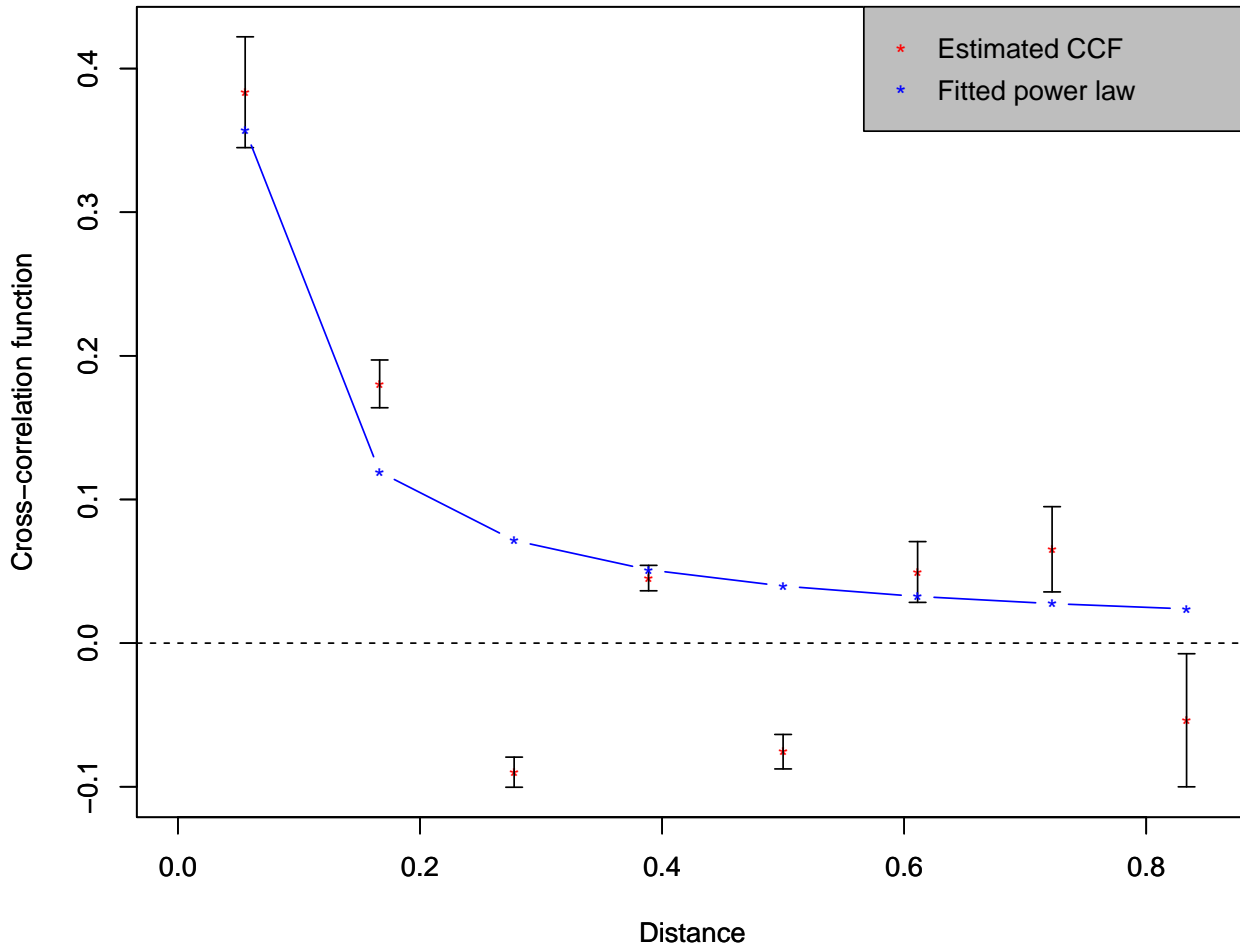
Fig. 9 CCF plot for the representative sample of the outermost part of nearby ETGs (data set 3) and the ETGs with $0.5 \leq z \leq 0.75$ (data set 4). The solid line represents the fitted power law $\xi(d) = 0.02d^{-1}$ and $p-$value= 0.66, corresponding to the Kolmogorov-Smirnov test for goodness of fit, indicates the fit is quite good.

Table 1 Compatibility test between two data sets in the
common redshift zone, using the parameters size, mass, RA_l
and DEC_l.

First data set	Second data set	z	No. of ETGs in two data sets	Parameter-wise $p-$values	Decision at 5% level of significance
Damjanov et al. (2011)	Papovich et al. (2012)	[1.49, 1.79]	(22, 248)	(1, 1, 0.413, 1)	Accept
"	Chen et al. (2013)	[0.703, 1.309]	(199, 142)	(1, 0.998, 1, 1)	Accept
"	Szomoru et al. (2013)	(0.5,2.7)	(364, 177)	(1, 1, 1, 1)	Accept
"	McLure et al. (2013)	[1.280, 1.505]	(36, 81)	(1, 1, 0.389, 1)	Accept